AJNR

Perfusion-sensitive MR Imaging of Gliomas: Comparison between Gradient-echo and Spin-echo Echo-planar Imaging Techniques

Takeshi Sugahara, Yukunori Korogi, Masato Kochi, Yukitaka Ushio and Mutsumasa Takahashi

AJNR Am J Neuroradiol 2001, 22 (7) 1306-1315
http://www.ajnr.org/content/22/7/1306

AJNR Am J Neuroradiol 22:1306–1315, August 2001

Perfusion-sensitive MR Imaging of Gliomas: Comparison between Gradient-echo and Spin-echo Echo-planar Imaging Techniques

Takeshi Sugahara, Yukunori Korogi, Masato Kochi, Yukitaka Ushio, and Mutsumasa Takahashi

BACKGROUND AND PURPOSE: **The different sensitivities to vessel size of gradient-echo echo-planar imaging (GE-EPI) and spin-echo EPI (SE-EPI) might indicate the relative cerebral blood volumes (rCBVs) of different tumor sizes. The techniques of GE-EPI and SE-EPI were compared for detecting low- versus high-grade gliomas.**

METHODS: **Six patients with low-grade gliomas and 19 patients with high-grade gliomas underwent two perfusion-sensitive MR procedures, one produced by a GE- and the other by an SE-EPI technique. Maximum rCBV ratios normalized with rCBV of contralateral white matter were calculated for evaluation. $P < .05$ was considered statistically significant.**

RESULTS: **Maximum rCBV ratios of high-grade gliomas obtained with the GE-EPI technique (mean, 5.0 ± 2.9) were significantly higher than those obtained with the SE-EPI technique (mean, 2.9 ± 2.3) ($P = .02$). Maximum rCBV ratios of low-grade gliomas obtained with the GE-EPI technique (mean, 1.2 ± 0.7) were almost equal to those obtained with the SE-EPI technique (mean, 1.2 ± 0.6), and there was no significant difference ($P = .66$). The difference in the maximum rCBV ratios between the low- and high-grade gliomas reached significance when obtained with the GE-EPI technique ($P = .01$).**

CONCLUSION: **The GE-EPI technique seems more useful for detecting low- versus high-grade gliomas than the SE-EPI technique.**

The principles underlying the susceptibility of contrast phenomena are highly dependent on the specific acquisition technique used. Numerical techniques have been applied to predict the response of both transverse relaxation rates ($\Delta R2$) for T2-weighted spin-echo (SE) and those ($\Delta R2^*$) for gradient-echo (GE) techniques (1–3). These previous studies showed that as vessel size increased, $\Delta R2$ increased and peaked for vessels of 1 to 2 μm, whereas $\Delta R2^*$ increased then plateaued to remain independent of vessel size beyond 3 to 4 μm. Because of this sensitivity to the microvasculature, T2-weighted SE techniques have been used for the evaluation of tumor vessels at the capillary level, which might be consistent with histologic tumor vessel evaluation, and also for grading systems such as gliomas (4, 5).

Received September 6, 2000; accepted after revision March 19, 2001.

From the Departments of Radiology (T.S., Y.K., M.T.) and Neurosurgery (M.K., Y.U.), Kumamoto University School of Medicine, Kumamoto, Japan.

Address reprint requests to Takeshi Sugahara, MD, Department of Radiology, Kumamoto University School of Medicine, 1-1-1 Honjo, Kumamoto 860-8556 Japan.

The vasculature of tumors is, however, very complex compared with that of normal tissues (6). For example, the tumor vasculature of the malignant gliomas typically consists of two types of vessels. The first type is derived from existing anatomic vessels taken over by the tumor for its arterial supply and venous drainage. These vessels may become tortuous, possibly because of more rapid blood flow or adjacent pressures of tumor growth, necrosis, or edema (6). The second type of vascular formation is made up of new vessels induced by or developed for tumor growth. This vasculature mainly consists of wild tangles and irregular meshworks of vessels in viable portions of a tumor (6). Additionally, the arteriovenous anastomoses and aneurysmal dilatation of vessels are developed in viable portions of a tumor (6).

We previously (7) found that the mean maximum relative cerebral blood volume (rCBV) ratios of high-grade gliomas obtained with GE echo-planar imaging (GE-EPI) were 1.6-fold higher than those obtained with the SE-EPI technique (4). These differences might result from the findings that the average vessel size of a tumor is greater than that of capillaries and that the GE-EPI technique is sensitive to those larger vessels. We, therefore, performed perfusion-sensitive MR imaging with both

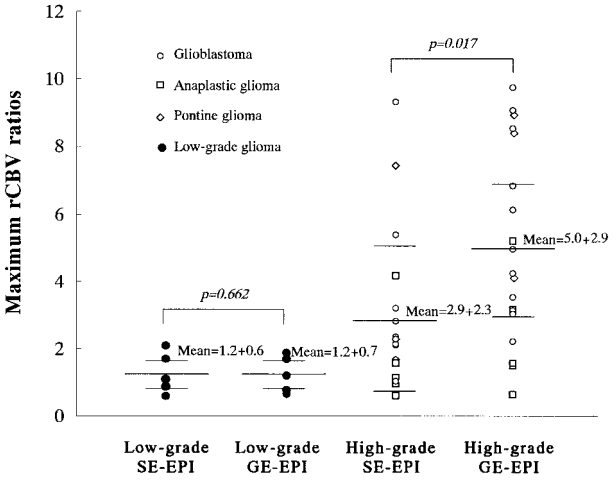

FIG 1. Relationship of the maximum rCBV of the low- and high-grade gliomas between the GE- (2000/46/1 [TR/TE/excitation]) and the SE-EPI (2000/97/1) techniques. For high-grade gliomas, the maximum rCBV ratios obtained with GE-EPI are significantly higher than those acquired with SE-EPI, whereas there is no significant difference for low-grade gliomas.

SE- and GE-EPI techniques in patients with gliomas and evaluated which technique was more sensitive for detecting low- versus high-grade gliomas.

Methods

Patients

Twenty-five consecutive patients with intraaxial gliomas were prospectively entered into the study over a 15-month period between December 1997 and March 1999. There were 15 male and 10 female patients, who ranged in age from 13 to 68 years (mean, 41 ± 18 years). Surgical resection or stereotactic biopsy verified the gliomas of 22 patients. The remaining three young patients with pontine tumors did not undergo biopsy, because biopsy posed a risk of neurologic deficits, and the diagnoses were obtained from the findings that the patients had progressive clinical deterioration and that conventional MR images showed the swelling and diffuse involvement of the brain stem, which is typical for pontine gliomas. The tumor specimens obtained were examined by a neuropathologist and graded according to the World Health Organization classification revised in 1993 and the grading system of Daumas-Duport et al (8, 9); grade 2 tumors were designated as low-grade gliomas, and grade 3 and 4 tumors as high-grade gliomas. The three pontine gliomas, from which no histologic specimens were obtained, were grouped as high-grade gliomas because brain stem tumors often result in a poor outcome, especially in patients with a short history of symptoms (10, 11). Therefore, the final diagnoses were classified as six low-grade gliomas (six astrocytomas) and 19 high-grade glial tumors (12 glioblastomas, three anaplastic astrocytomas, one anaplastic oligodendroglioma, and three pontine gliomas). There were no grade 1 gliomas.

Imaging

All MR images were obtained using a 1.5-T superconducting system. Conventional MR images and perfusion-sensitive MR images obtained with GE- and SE-EPI techniques were acquired during the same procedure to allow an exact comparison of the findings. For all patients, perfusion-sensitive MR images with the GE-EPI technique were obtained at a readout bandwidth of 926 Hz per pixel, maximum amplitude of 25 mT/m, at 2000/46/1 (TR/TE/excitation); those with the SE-EPI technique were obtained at a readout bandwidth of 926 Hz per pixel, maximum amplitude of 25 mT/m, at 2000/97/1. Sagittal T1-weighted localizing images were acquired first. Unenhanced axial T1- and T2-weighted images were then obtained for each patient. Before the recording of perfusion-sensitive MR imaging, a 21-gauge intravenous needle was inserted in the vein of the right antecubital fossa. Axial sections were selected from the unenhanced images for dynamic MR imaging. After 0.01 mmol/kg of contrast medium was injected to minimize the effect of T1 shortening from enhancing lesions, a 0.07-mmol/kg bolus of gadopentetate dimeglumine was injected with a mechanical injection pump (3 mL/s), followed by a 20-mL saline flush. To minimize the difference in T1 shortening effects, the SE- and GE-EPI techniques were performed in random order.

In the present study, a series of images was obtained using a lipid-suppressed EPI technique before, during, and after the injection of each contrast agent (12). Lipid suppression was used to suppress subcutaneous fat, which can be superimposed on the brain because of a large chemical shift in artifacts seen with EPI. All patients were studied with multisection data acquisition to record the tumors in their entirety. For all patients, 30 images were obtained at each section location during 60-second periods separated by 2-second intervals. Each section was collected using a section thickness of 5 mm, an intersection gap of 1 mm, a 256 × 128 matrix, and a field of view of 20 × 22–28 cm. After data collection, the rCBV maps were derived on a voxel-by-voxel basis from the dynamic image sets.

The start and end points of the first-pass transit of the contrast agent through the brain were identified using the time-activity curve of the means of the signal magnitude of the pixels covering the whole-brain tissue on the section. Before the starting point of the first-pass circulation (seen as a drop in the signal), a representative number of baseline points were selected and their average was calculated for each pixel as a baseline measure for signal intensity (So). On a pixel-by-pixel basis, the signal intensity (S) was converted to changes in the T2* relaxation rate (ΔR2*); $\Delta R2^* = -\ln(S/So)/TE$. Previous experiments and theoretical calculations have demonstrated that ΔR2* is approximately linearly proportional to the concentration of the contrast material in the tissue (13). The rCBV maps were generated by the numerical integration of the relative concentration (ΔR2*) for the first-pass bolus through each voxel on the basis of kinetic principles for nondiffusible tracers (14, 15). The imaging process required approximately 20 minutes to integrate the functional time course data.

Since the rCBV mapping method yields a relative rather than an absolute value of CBV, the comparison of the patients was facilitated by reference to an internal contralateral standard. As in a positron emission tomography study (16), the normal white matter in the contralateral hemisphere was used as a reference. For the calculation of the maximum rCBV ratios of tumor to white matter, the regions of interest (ROIs) consisting of more than 20 pixels were carefully chosen by a radiologist (T.S.) who was blinded to the clinical diagnosis. To avoid the risk of calculating the rCBV from normal vessels such as cerebral arteries and veins, the radiologist initially investigated the serial ΔR2* maps from arterial to venous phases as well as conventional MR images and then located the ROIs within the tumors. The ΔR2* maps clearly demonstrated the rCBV values from cerebral arteries or veins (7), and the ROIs were easily defined without the superimposition of those vessels. When a glial tumor showed enhanced areas within the tumor on the contrast-enhanced T1-weighted images, the ROIs were located at visually higher rCBV areas within both enhanced and unenhanced areas. When a glial tumor had no enhanced areas, the ROIs also were located at visually higher rCBV areas within the tumors. The ROIs were located at least

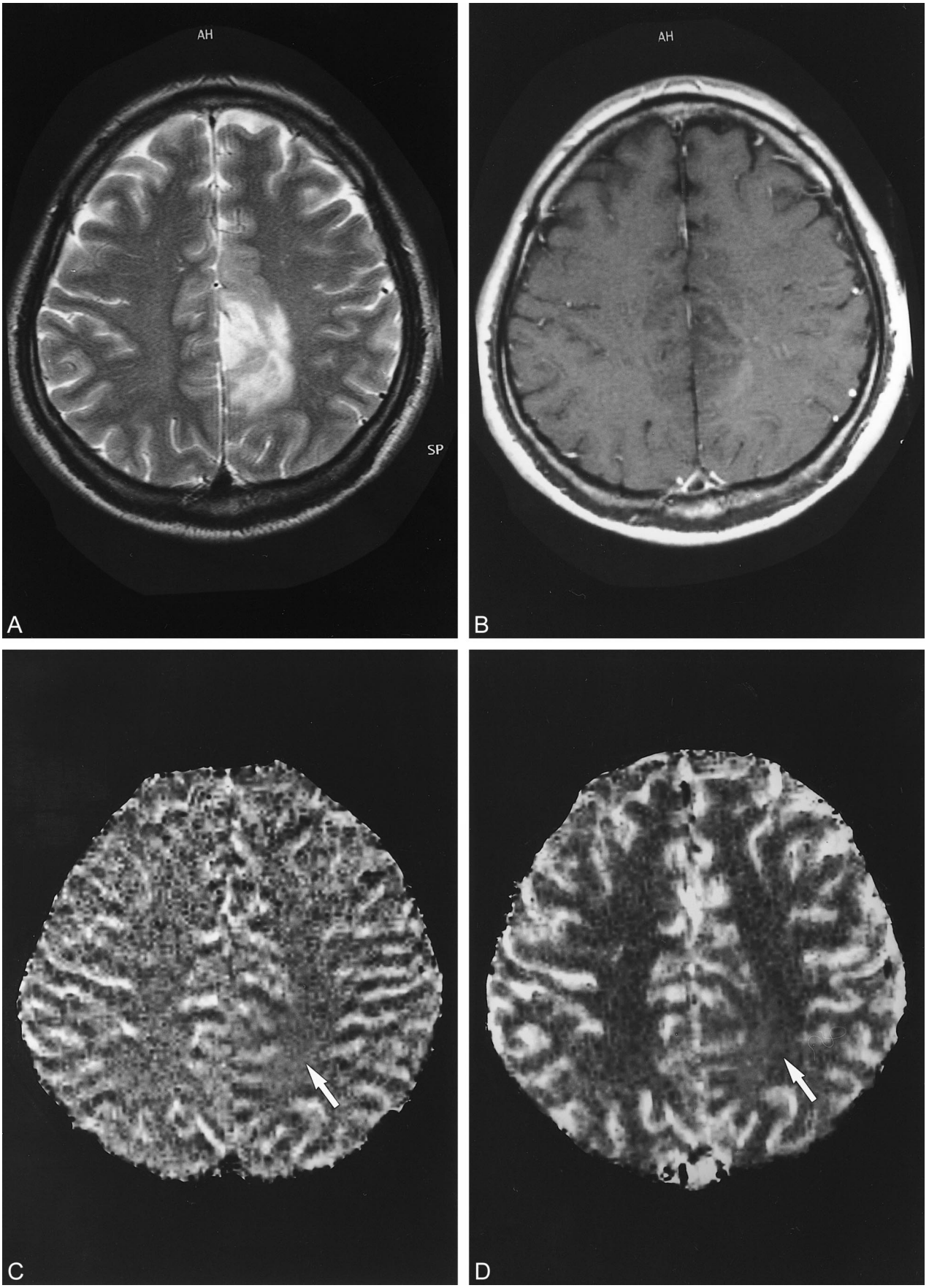
AH
SP
A
AH
B
C
D

five times in each enhanced and unenhanced area, and rCBV values were calculated.

Data Analysis

The relationship of the tumor grade to the maximum rCBV ratios in each GE- and SE-EPI technique was analyzed using Student's *t* test. The difference in the maximum rCBV ratios between the two techniques in each low- and high-grade glioma also was analyzed using Student's *t* test. $P < .05$ was considered statistically significant.

Plots of maximum rCBV ratios obtained with GE-EPI versus those obtained with SE-EPI were made for each low- and high-grade glioma. The relationship of the maximum rCBV between the two techniques was analyzed using simple linear regression analysis.

Results

Five low-grade gliomas, three pontine gliomas, and one anaplastic glioma did not have tumor enhancement, and the others did. Tumor grade was correlated with tumor enhancement ($r = 0.969$, $P < .001$).

With the SE-EPI technique, the maximum rCBV ratios of the low-grade gliomas ranged from 0.54 to 2.13 (mean ± SD = 1.22 ± 0.70). The maximum rCBV ratios of the high-grade gliomas obtained with the SE-EPI technique ranged from 0.56 to 9.30 (mean ± SD = 2.90 ± 2.32). The maximum rCBV ratios of high-grade gliomas were higher than those of low-grade gliomas, but the difference did not reach statistical significance ($P = .06$). Tumor grade was correlated with the maximum rCBV ratios obtained with the SE-EPI technique ($r = 0.798$, $P < .001$).

With the GE-EPI technique, the maximum rCBV ratios of the low-grade gliomas ranged from 0.43 to 1.34 (mean ± SD = 1.21 ± 0.67). The maximum rCBV ratios of the high-grade gliomas ranged from 0.61 to 9.71 (mean ± SD = 4.86 ± 2.93). The maximum rCBV ratios of the high-grade gliomas were significantly higher than those of the low-grade gliomas ($P = .013$). Tumor grade also was correlated with the maximum rCBV ratios obtained with the GE-EPI technique ($r = 0.862$, $P < .001$).

In the low-grade gliomas, there were no significant differences in the maximum rCBV ratios between the GE- and SE-EPI techniques ($P = .662$) (Figs 1 and 2). In the high-grade gliomas, the maximum rCBV ratios obtained with the GE-EPI technique were significantly higher than those acquired with the SE-EPI technique ($P = .017$) (Figs 1 and 3). The rCBV map obtained with the GE-EPI technique more clearly showed the areas of high rCBV within the tumor than that obtained with the SE-EPI technique (Fig 4). In all high-grade gliomas, the values of rCBV obtained with the GE-EPI technique were consistently higher than those acquired with the SE-EPI technique (Fig 5).

It is of interest that, in some patients with high-grade gliomas, the susceptibility effects within the tumors had not completely disappeared after the first pass of the contrast medium on the GE-EPI, whereas those of normal white matter had completely disappeared (Fig 6). However, these phenomena were not observed in the patients with low-grade gliomas.

Discussion

Along with increased vasculature, tumor vessels are associated with a distinct range of both morphologic and physiologic properties that are not present in normal tissue vasculature (6). Qualitatively, tumor vessels are disordered and dominated by large, dilatated, and tortuous vascular structures with increased vessel spacing. Deane and colleagues (17) studied the various phases of vascularization of rat glioma and discovered that, during the late phase of growth, microvessels with diameters of 40 μm could be found in the intermediate zone of the tumor, the zone between the necrotic core and the proliferating edge. These vessels also varied in shape and size. Using scanning electron microscopy on tumor vascular casts, Zama et al (18) assessed the three-dimensional growth patterns of rat gliomas. They found large, budding vessels that attained diameters of 250 μm. These buds, although filled with blood, did not have normal blood flow characteristics. However, the method of evaluation was invasive and did not reproduce the heterogeneity inherent to tumors.

Recently, Dennie et al (19) studied the vasculature of C6 rat gliomas with susceptibility contrast MR imaging by use of GE and SE techniques, and found the measured tumor ratio of ΔR2* to ΔR2 to be a factor 1.9-fold greater than the ratio of normal gray matter. These findings suggest that tumor vascular morphology can be assessed in vivo with the use of a combination of perfusion-sensitive MR imaging based on ΔR2* and ΔR2. However, because the size of vessels within a tumor in the human brain varies with the aggressiveness of the tumor and because the contrast medium used by Dennie et al (an intravascular contrast agent, monocrystalline iron oxide nanoparticles, known as MION) cannot yet be used in human studies, it is

←

FIG 2. A 35-year-old man with low-grade astrocytoma.

A, T2-weighted image at 3700/96/1 (TR/TE/excitation). Left frontoparietal tumor with hyperintensity is not enhanced after contrast medium administration.

B, Contrast-enhanced T1-weighted image at 690/14/1.

C and *D,* SE-EPI at 2000/97/1 (*C*) and GE-EPI (*D,*) at 2000/46/1. On the perfusion-sensitive MR imaging, tumor CBV (*arrow*) is lower than that of gray matter obtained with the two techniques.

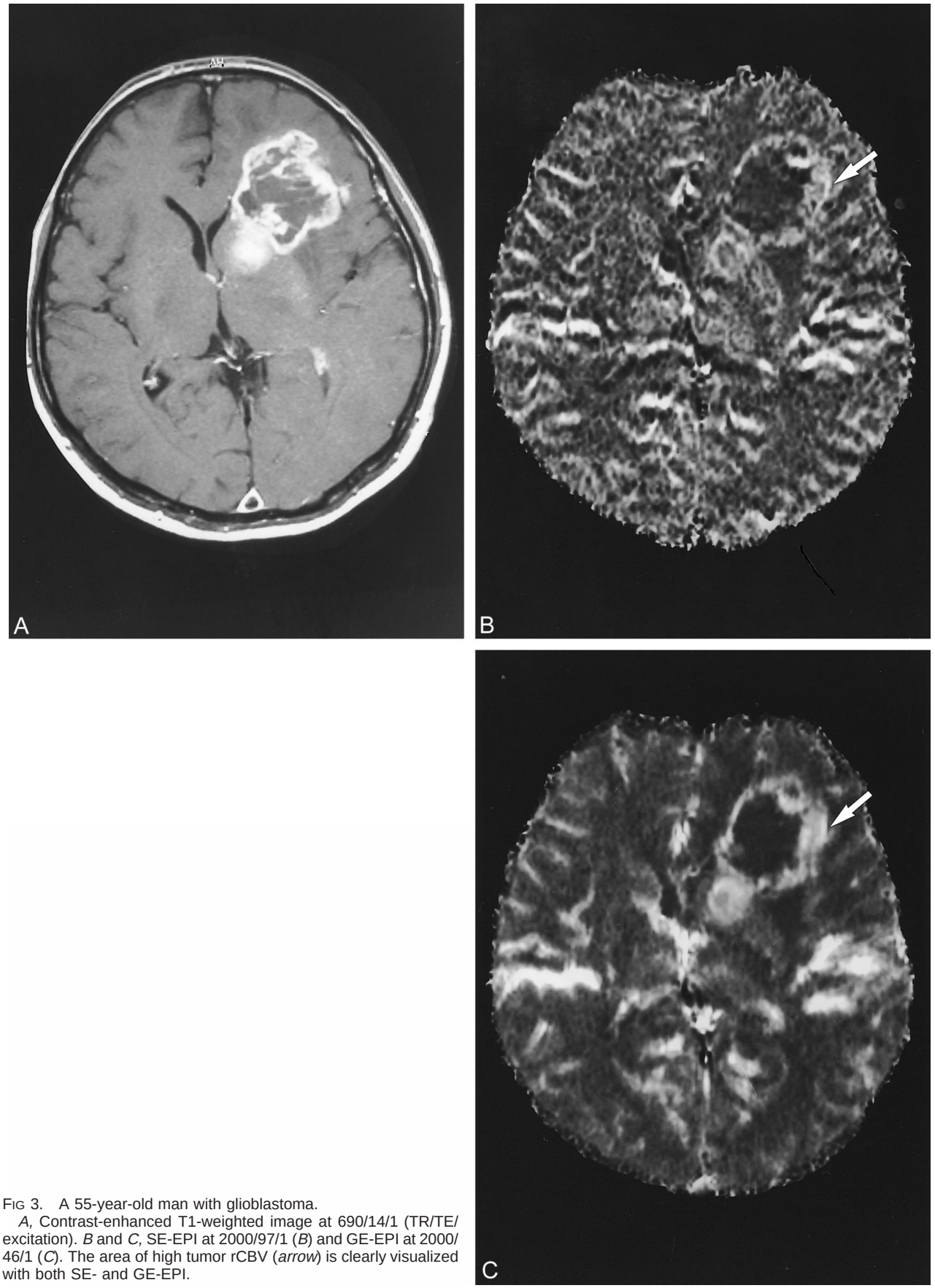

FIG 3. A 55-year-old man with glioblastoma.

A, Contrast-enhanced T1-weighted image at 690/14/1 (TR/TE/excitation). *B* and *C,* SE-EPI at 2000/97/1 (*B*) and GE-EPI at 2000/46/1 (*C*). The area of high tumor rCBV (*arrow*) is clearly visualized with both SE- and GE-EPI.

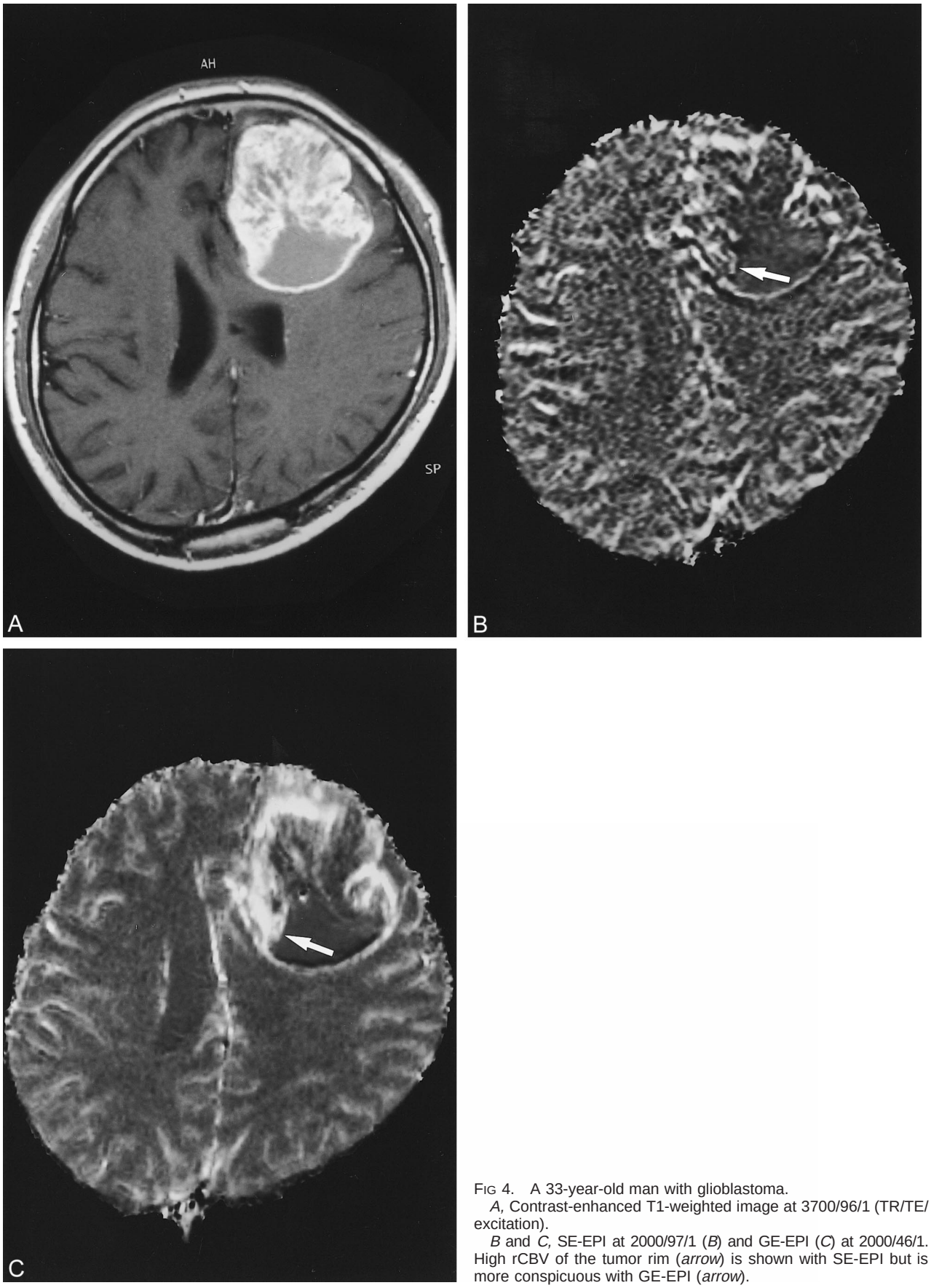

FIG 4. A 33-year-old man with glioblastoma.

A, Contrast-enhanced T1-weighted image at 3700/96/1 (TR/TE/excitation).

B and *C,* SE-EPI at 2000/97/1 (*B*) and GE-EPI (*C*) at 2000/46/1. High rCBV of the tumor rim (*arrow*) is shown with SE-EPI but is more conspicuous with GE-EPI (*arrow*).

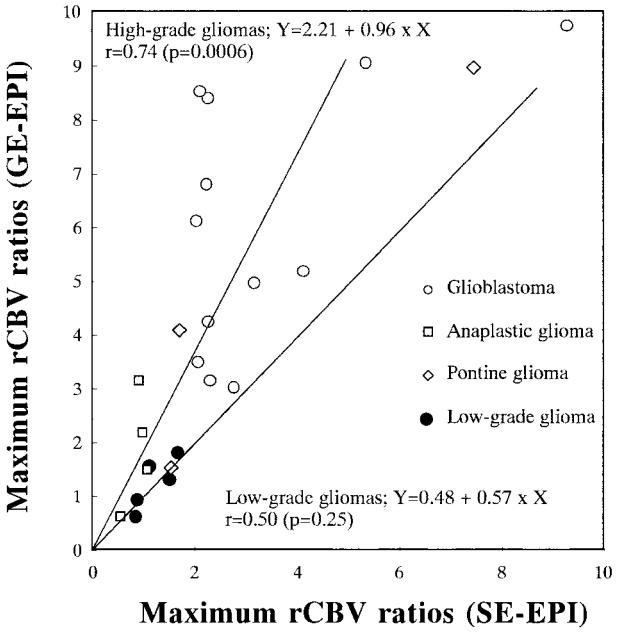

FIG 5. The maximum rCBV ratios calculated with the GE-EPI technique at 2000/46/1 (TR/TE/excitation) versus those obtained with SE-EPI at 2000/97/1.

unknown whether the findings are applicable to human brain tumors.

In the present study, we show that the maximum rCBV ratios of high-grade gliomas obtained from the GE-EPI technique were significantly higher than those acquired from the SE-EPI technique, and that the significant difference between the high-grade and low-grade gliomas were obtained only with the GE-EPI technique. These findings are important because the larger tumor vessels that are essential for the characterization of tumor vasculature could be detected only with the GE-EPI technique. Indeed, the tumor rCBV ratios obtained by using the GE-EPI technique were consistently higher than those derived from the SE-EPI technique. In other words, the SE-EPI technique's specific sensitivity to small vessels allows the risk of underestimating the tumor rCBV.

However, the maximum rCBV ratios of low-grade gliomas did not differ between the two techniques. It has been suggested that the sizes of vessels within a tumor vary with the aggressiveness of the tumor (20). Low-grade gliomas, which have been known not to be associated with as dramatic an increase in blood volume as high-grade gliomas, might not exhibit the corresponding increase in vessel diameter. Therefore, the tumor rCBV obtained primarily reflected the susceptibility from small vessels at the capillary level, and the tumor rCBV based on GE-EPI was not significantly higher than that based on the SE-EPI technique for low-grade glioma.

As stated earlier, from the difference of tumor vessel size, the ratio of tumor rCBV based on GE-EPI to that based on SE-EPI was also different between low-grade and high-grade gliomas. Dennie et al (19) have shown that, from the direct histologic measurements, the relative diameter of the average tumor vessel compared with the average gray matter vessel was the same as the ratio of $\Delta R2^*$ and $\Delta R2$ between these tissues. Although this ratio of $\Delta R2^*$ and $\Delta R2$ is not necessarily applied to the ratio of tumor rCBV based on GE-EPI to that based on SE-EPI (19), these findings suggest the possibility that the average vessel size within a tumor could be predicted with the use of both the GE-EPI and SE-EPI techniques. To validate our hypothesis, more detailed investigations are needed.

In some high-grade gliomas, the susceptibility effects within tumors did not completely disappear after the first pass of the contrast medium. It is suggested that these phenomena result from the following factors. First, Yuan et al (21) found that the red blood cell velocity in pial vessels might be significantly faster than that in tumor vessels of the same diameter (ie, flow velocity within tumor vessels might be lower than that within normal brain tissue and, thus, residual susceptibility effects could be observed). Second, the susceptibility effects were produced not only between intravascular and extravascular space but also within extravascular space near the disrupted blood-brain barrier. Generally, the enhancing lesion produces T1 shortening effects, which are considered to cause the underestimation of the true rCBV (22). However, on the condition of bolus injection, rapidly leaking contrast medium would be concentrated enough to produce a susceptibility effect between leaked and nonleaked tissues. In the present study, the GE-EPI technique was more sensitive to these phenomena, and it is suggested that it might express the specific tumor vasculature as mentioned earlier.

Attention should be given to the choice of areas of maximum rCBV when the GE-EPI technique is used for the rCBV maps. Because the GE-EPI technique is sensitive to susceptibility effects from total vascular beds, normal arteries and veins located at the surface of the brain tissue and ventricles might be misunderstood as tumor vascularity. If highly vascular areas within the gliomas are located adjacent to the surface of brain tissues, the identification of areas of maximum rCBV of gliomas might be difficult. However, it is possible to avoid confusion between gliomas and normal brain tissue with a detailed investigation of serial $\Delta R2^*$ maps as well as conventional MR imaging.

There are limitations to our findings. First, the SE-EPI technique used maintains some sensitivity to very large vessels such as the middle cerebral artery (2, 23). The conventional SE technique has been illustrated to be specifically sensitive to the microvasculature at the capillary level (24). However, this principle is not necessarily applied to the EPI technique. Therefore, we could not say that the difference in tumor rCBV ratios between GE- and SE-EPI techniques only represented the difference in tumor vascular size between capillary and larger vessels. Second, al-

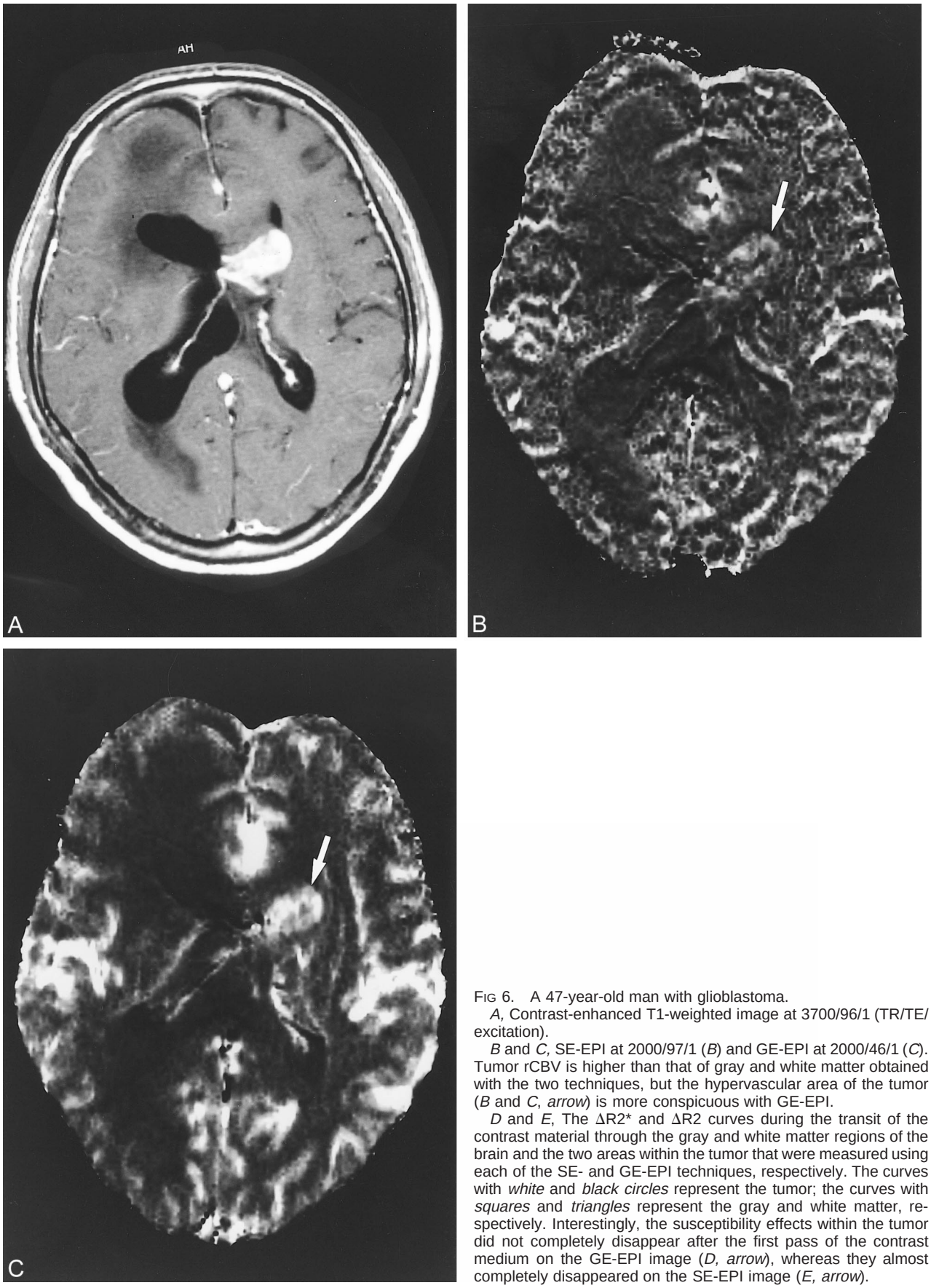

FIG 6. A 47-year-old man with glioblastoma.

A, Contrast-enhanced T1-weighted image at 3700/96/1 (TR/TE/excitation).

B and *C,* SE-EPI at 2000/97/1 (*B*) and GE-EPI at 2000/46/1 (*C*). Tumor rCBV is higher than that of gray and white matter obtained with the two techniques, but the hypervascular area of the tumor (*B* and *C*, *arrow*) is more conspicuous with GE-EPI.

D and *E*, The $\Delta R2^*$ and $\Delta R2$ curves during the transit of the contrast material through the gray and white matter regions of the brain and the two areas within the tumor that were measured using each of the SE- and GE-EPI techniques, respectively. The curves with *white* and *black circles* represent the tumor; the curves with *squares* and *triangles* represent the gray and white matter, respectively. Interestingly, the susceptibility effects within the tumor did not completely disappear after the first pass of the contrast medium on the GE-EPI image (*D, arrow*), whereas they almost completely disappeared on the SE-EPI image (*E, arrow*).

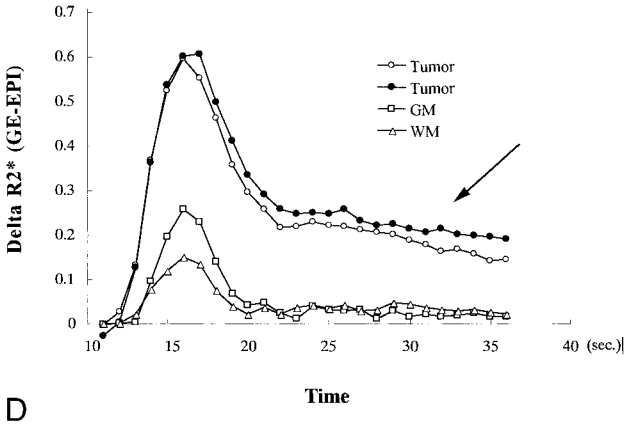

D

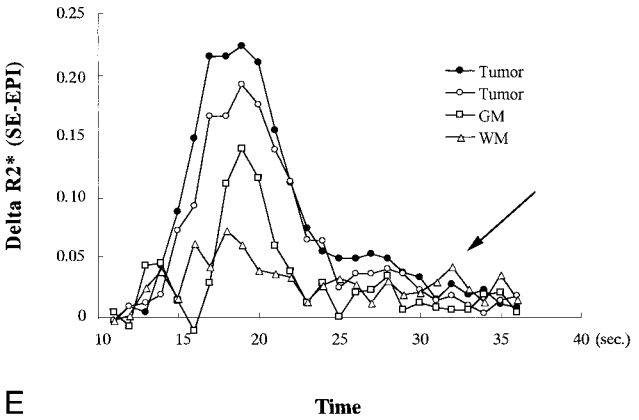

E

FIG 6. Continued.

though the 0.01 mmol/kg of contrast agent was injected before the perfusion-sensitive MR imaging, the total volume was small and the T1 shortening effect from the extravascular space accumulated during the first pass could not be completely excluded. In a study by Donahue et al (25), a strong correlation between the rCBV obtained with the GE-EPI and the tumor grade was only significant when the rCBV values were mathematically corrected for T1 leakage effects by postprocessing. Since we also observed a correlation between the rCBV with the GE-EPI and tumor grade, it is suggested that the present small ''pre'' dose of gadopentetate dimeglumine can still correct for T1-leakage effect. Third, for economic reasons, we used only 0.07 mmol/kg of contrast medium for the SE-EPI technique in each patient, which degraded the image quality of perfusion-sensitive MR and might have affected the tumor rCBV ratios (2). Optimized rCBV maps of high-grade gliomas obtained with the SE-EPI technique might show higher rCBV values than was demonstrated by the present study. Finally, the SE- and GE-EPI techniques were performed in random order to compare the two techniques under the same conditions, but this method could not exclude the different T1 shortening effects between the two techniques, because the degree of tumor enhancement caused by the leakage of contrast material was different in each glioma. To overcome these problems, more detailed and systematic evaluations are needed.

Conclusion

The tumor rCBV obtained with the GE-EPI technique was significantly higher than that obtained with the SE-EPI technique in the high-grade gliomas, but not in the low-grade gliomas. These findings must have been produced by the higher sensitivity of the GE-EPI technique to large vessels, which can be clearly observed in the high-grade gliomas. The findings suggest that the GE-EPI technique is more useful for detecting low- versus high-grade gliomas than is the SE-EPI technique.

References

1. Ogawa S, Menon RS, Tank DW, et al. **Functional brain mapping by blood oxygenation level-dependent contrast magnetic resonance imaging: a comparison of signal characteristics with a biophysical model.** *Biophys J* 1993;64:803–812
2. Kennan RP, Zhong J, Gore JC. **Intravascular susceptibility contrast mechanisms in tissues.** *Magn Reson Med* 1994;31:9–21
3. Fisel CR, Ackerman JL, Buxton RB, et al. **MR contrast due to microscopically heterogeneous magnetic susceptibility: numerical simulations and applications to cerebral physiology.** *Magn Reson Med* 1991;17:336–347
4. Aronen HJ, Gazit IE, Louis DN, et al. **Cerebral blood volume maps of gliomas: comparison with tumor grade and histologic findings.** *Radiology* 1994;191:41–51
5. Bruening R, Kwong KK, Vevea MJ, et al. **Echo-planar MR determination of relative cerebral blood volume in human brain tumors: T1 versus T2 weighting.** *AJNR Am J Neuroradiol* 1996; 17:831–840
6. Scatliff JH, Radcliffe WB, Pittman HH, Park CH. **Vascular structure of glioblastomas.** *Am J Roentgenol Radium Ther Nucl Med* 1969;105:795–805
7. Sugahara T, Korogi Y, Kochi M, et al. **Correlation of MR imaging-determined cerebral blood volume maps with histologic and angiographic determination of vascularity of gliomas.** *AJR Am J Roentgenol* 1998;171:1479–1486
8. Kleihues P, Burger PC, Scheithauer BW. ***Histological Typing of Tumours of the Central Nervous System.*** **2nd ed.** Berlin: Springer-Verlag; 1993
9. Daumas-Duport C, Scheithauer B, O'Fallon J, Kelly P. **Grading of astrocytomas: a simple and reproducible method.** *Cancer* 1988;62:2152–2165
10. Prados MD, Wara WM, Edwards MSB, Larson DA, Lamborn K, Levin VA. **The treatment of brain stem and thalamic gliomas with 78 Gy of hyperfractionated radiation therapy.** *Int J Radiat Oncol Bio Phys* 1993;27:197–206
11. Lewis J, Lucraft H, Gholkar A. **UKCCSG study of accelerated radiotherapy for pediatric brain stem gliomas.** *Int J Radiat Oncol Bio Phys* 1997;38:925–929
12. Rosen BR, Aronen HJ, Kwong KK, Belliveau JW, Hamberg LM, Fordham JA. **Advances in clinical neuroimaging: functional MR imaging techniques.** *Radiographics* 1993;13:889–896
13. Weisskoff R, Belliveau J, Kwong K, Rosen B. **Functional MR imaging of capillary hemodynamics.** In: Potchen E, ed. *Magnetic Resonance Angiography: Concepts and Applications.*Vol 14. St. Louis, Mo: Mosby; 1992:538–546
14. Axel L. **Cerebral blood flow determination by rapid-sequence computed tomography: a theoretical analysis.** *Radiology* 1980; 137:679–686

15. Villringer A, Rosen BR, Belliveau JW, et al. **Dynamic imaging with lanthanide chelates in normal brain: contrast due to magnetic susceptibility effects.** *Magn Reson Med* 1988;6:164–174
16. Majumdar S, Gore JC. **Effects of selective pulses on the measurement of T2 and apparent diffusion in multiecho MRI.** *Magn Reson Med* 1987;4:120–128
17. Deane BR, Papp MI, Lantos PL. **The vasculature of experimental brain tumours, III: permeability studies.** *J Neurol Sci* 1984; 65:47–58
18. Zama A, Tamura M, Inoue HK. **Three-dimensional observations on microvascular growth in rat glioma using a vascular casting method.** *J Cancer Res Clin Oncol* 1991;117:396–402
19. Dennie J, Mandeville JB, Boxerman JL, Packard SD, Rosen BR, Weisskoff RM. **NMR imaging of changes in vascular morphology due to tumor angiogenesis.** *Magn Reson Med* 1998;40: 793–799
20. Papadimitrou JM, Woods AE. **Structural and functional characteristics of the microcirculation in neoplasms.** *J Pathol* 1975; 116:65–72
21. Yuan F, Salehi HA, Boucher Y, Vasthare US, Tuma RF, Jain RK. **Vascular permeability and microcirculation of gliomas and mammary carcinomas transplanted in rat and mouse cranial windows.** *Cancer Res* 1994;54:4564–4568
22. Uematsu H, Maeda M, Sadato N, et al. **Vascular permeability: quantitative measurement with double-echo dynamic MR imaging—theory and clinical application.** *Radiology* 2000;214: 912–917
23. Hamberg LM, Macfarlane R, Tasdemiroglu E, et al. **Measurement of cerebrovascular changes in cats after transient ischemia using dynamic magnetic resonance imaging.** *Stroke* 1993; 24:444–450
24. Boxerman JL, Hamberg LM, Rosen BR, Weisskoff RM. **MR contrast due to intravascular magnetic susceptibility perturbations.** *Magn Reson Med* 1996;34:555–566
25. Donahue KM, Krouwer HGJ, Rand SD, et al. **Utility of simultaneously acquired gradient-echo and spin-echo cerebral blood volume and morphology maps in brain tumor patients.** *Magn Reson Med* 2000;43:845–853